Journal of
Computational and Theoretical Nanoscience
Vol. 11, 1–8, 2014

The Effect of Rotation and Initial Stress on Thermal Shock Problem for a Fiber-Reinforced Anisotropic Half-Space Using Green-Naghdi Theory

Ibrahim A. Abbas[1, 2, *] and Ashraf M. Zenkour[3]

[1] *Faculty of Science, Department of Mathematics, Sohag University, Sohag, Egypt*
[2] *Faculty of Science and Arts—Khulais, Department of Mathematics, King Abdulaziz University, Jeddah, Saudi Arabia*
[3] *Faculty of Science, Department of Mathematics, King Abdulaziz University, P.O. Box 80203, Jeddah 21589, Saudi Arabia*

This article presents a two-dimensional problem of generalized thermoelasticity for a fiber-reinforcement anisotropic half-space under a thermal shock at its upper surface. The effects of initial stress and rotation are both studied. Green and Naghdi's theory of thermoelasticity is employed to study the present problem. The inclusion of reinforcement anisotropic elastic parameter is made and two additional terms are added to the displacement equation. The problem is solved numerically by using the finite element method. Numerical results for displacements, stresses and temperature are given and presented graphically in different positions. Comparisons are made for different values of the angular velocity and initial stress. The inclusion of the reinforcement parameters is also investigated.

Keywords: Thermomechanical, Finite Element Analysis, Strength, Green and Naghdi's Theory, Fiber-Reinforced, Finite Element Method.

RESEARCH ARTICLE

1. INTRODUCTION

The problem of a half-space subjected to a thermal shock in the context of the theory of uncoupled thermoelasticity is solved firstly by Danilovskaya.[1] In the uncoupled thermoelasticity theory the temperature is governed by a parabolic partial differential equation which does not contain any elastic terms. So, the elastic changes have no effect on the temperature. It was not much latter that many attempts were made to remedy the shortcomings of this theory. Biot[2] formulated the theory of coupled thermoelasticity to eliminate the paradox inherent in the classical uncoupled theory. The heat equations for both theories, however, are of the diffusion type predicting infinite speeds of propagation for heat waves contrary to physical observations.

The theory of thermoelasticity that includes the effect of temperature change has been well established. According to this theory, the temperature field is coupled with the elastic strain field. This theory covers a wide range of extensions of classical dynamical coupled thermoelasticity. Lord and Shulman[3] and Green and Lindsay[4] extended the coupled theory of thermoelasticity by introducing the thermal relaxation times in the constitutive equations. Additional thermoelasticity theories have been presented and investigated by other researchers.[5–12]

Lord and Shulman[3] considered isotropic solids and introduced one relaxation time parameter into the Fourier heat conduction equation; that is, both the heat flux and its time derivative are considered in the heat conduction equation. The heat equation associated with this theory is thus hyperbolic. A direct consequence is that the paradox of infinite speed of propagation inherent in both the uncoupled and coupled theories of classical thermoelasticity is eliminated and the heat wave feature can be modeled by the generalized thermoelasticity. Green and Lindsay[4] developed a temperature-rate dependent thermoelasticity which does not violate the Fourier's law of heat conduction when the body under consideration has a center of symmetry. In this theory, both the equations of motion and heat conduction are hyperbolic but the equation of motion is modified and differs from that of classical coupled thermoelasticity theory. Green and Naghdi[9] provided sufficient basic modifications in the constitutive equations to permit treatment of a much wider class of heat flow problem.

*Author to whom correspondence should be addressed.

Fiber-reinforced materials have many applications in aerospace and automotive fields, as well as in sailboats, and notably in modern bicycles and motorcycles, where their high strength-to-weight ratio is of importance. Improved manufacturing techniques are reducing the costs and time to manufacture, making it increasingly common in small consumer goods as well, such as laptops, tripods, fishing rods, paintball equipment, archery equipment, racquet frames, stringed instrument bodies, and classical guitar strings. Hashin and Rosen[13] gave the elastic moduli for fiber-reinforced materials. Sengupta and Nath[14] discussed the problem of surface waves in fiber-reinforced anisotropic elastic media. Singh[15] showed that, for wave propagation in fiber-reinforced anisotropic media, this decoupling cannot be achieved by the introduction of the displacement potentials.

The one-dimensional thermal shock problem has been considered by Sherief and Dhaliwal[16] using Lord and Shulman's theory. The same thermal shock problem has been considered by Dhaliwal and Rokne[17] using Green and Lindsay's theory. Once again, the same thermal shock problem has been considered by Li and Dhaliwal[18] using Green and Naghdi's theory. In this paper, two-dimensional thermal-shock problem of a fiber-reinforcement anisotropic half-space is studied. The effect of both initial stress and rotation is investigated. The governing equations of medium are derived based upon Green and Naghdi's theory. The finite element solution for the coupled governing equations is obtained. Numerical results are provided to show the influence of the fiber-reinforcement parameters on the temperature, displacements and stresses.

2. FORMULATION OF THE PROBLEM

Let us consider the problem of a thermoelastic half-space ($x \geq 0$) such that its surface is subjected to a thermal shock which is a function of y and t. Thus, all quantities considered will be functions of the time t, and of the coordinates x and y. The medium is rotating uniformly with an angular velocity $\boldsymbol{\Omega} = \Omega \boldsymbol{n}$ in which $\boldsymbol{n}$ is a unit vector representing the direction of the axis of rotation. The components of the displacement vector u_i and temperature T can be taken in the following forms:

$$u_1 = u(x, y, t), \quad u_2 = v(x, y, t), \quad u_3 = 0 \qquad T = T(x, y, t) \tag{1}$$

According to Green and Nagdhi,[9] Singh[19] and Qian et al.[20] the linear equations governing thermoelastic interactions in the homogeneous anisotropic solid in the absence of body force and heat sources are given as follows:

$$\sigma_{ij,\,j} + (u_{i,\,k}\sigma^0_{kj})_{,\,j} = \rho[\ddot{u}_i + \{\boldsymbol{\Omega} \times (\boldsymbol{\Omega} \times \boldsymbol{u})\}_i + 2(\boldsymbol{\Omega} \times \dot{\boldsymbol{u}})_i] \qquad i, j = 1, 2, 3 \tag{2}$$

$$K^* T_{,ij} + K_{ij}\dot{T}_{,ij} = \rho c_e \ddot{T} + T_0 \ddot{u}_{i,\,j} \tag{3}$$

where ρ is the mass density; σ_{ij} is the stress tensor; σ^0_{kj} is the initial stress tensor; T_0 is the reference uniform temperature of the body; c_e is the specific heat at constant strain; K_{ij} is the thermal conductivity; and K^* is the material characteristic of the theory. The comma notation is used for spatial derivatives and superimposed dot represents time differentiation.

The constitutive equations for a linearly thermoelastic fiber-reinforced anisotropic medium whose preferred direction is that of a unit vector $\boldsymbol{a}$ is

$$\begin{aligned}\sigma_{ij} = {} & \lambda e_{kk}\delta_{ij} + 2\mu_T e_{ij} + \alpha(a_k a_m e_{km}\delta_{ij} + a_i a_j e_{kk}) \\ & + 2a_k(\mu_L - \mu_T)(a_i e_{kj} + a_j e_{ki}) + \beta a_k a_m e_{km} a_i a_j \\ & - \beta_{ij}(T - T_0)\delta_{ij}, \quad i, j, k, m = 1, 2, 3\end{aligned} \tag{4}$$

where e_{ij} is the strain tensor; δ_{ij} is Kronecker's delta; β_{ij} is the thermal elastic coupling tensor; λ and μ_T are Lamé's elastic parameters; α, β, and μ_L are additional reinforced anisotropic elastic parameters; and $\boldsymbol{a} \equiv (a_1, a_2, a_3)$, $a_1^2 + a_2^2 + a_3^2 = 1$.

The displacement equation of motion in the rotating frame of reference has two additional terms (Schoenberg and Censor[21]): Centripetal acceleration, $\boldsymbol{\Omega} \times (\boldsymbol{\Omega} \times \boldsymbol{u})$ due to time-varying motion only and the Corioli's acceleration $2(\Omega \times \dot{u})$. These terms should be disappearing in the non-rotating media. We choose the fiber-direction as $\boldsymbol{a} \equiv (1, 0, 0)$ so that the preferred direction is the x-axis and there exists only two constant initial stress components $\sigma^0_{11} = \sigma^0_{22} = \sigma_0$. So, Eqs. (2)–(4) may be simplified to be

$$(A_{11} + \sigma_0)\frac{\partial^2 u}{\partial x^2} + (A_{12} + \mu_L)\frac{\partial^2 v}{\partial x \partial y} + (\sigma_0 + \mu_L)\frac{\partial^2 u}{\partial y^2} = \beta_{11}\frac{\partial T}{\partial x} + \rho\frac{\partial^2 u}{\partial t^2} - \Omega^2 u - 2\Omega\frac{\partial v}{\partial t} \tag{5}$$

$$(A_{12} + \mu_L)\frac{\partial^2 u}{\partial x \partial y} + (\sigma_0 + \mu_L)\frac{\partial^2 v}{\partial x^2} + (A_{22} + \sigma_0)\frac{\partial^2 v}{\partial y^2} = \beta_{22}\frac{\partial T}{\partial y} + \rho\frac{\partial^2 v}{\partial t^2} - \Omega^2 v + 2\Omega\frac{\partial u}{\partial t} \tag{6}$$

$$\left(K^* + K_{11}\frac{\partial}{\partial t}\right)\frac{\partial^2 T}{\partial x^2} + \left(K^* + K_{22}\frac{\partial}{\partial t}\right)\frac{\partial^2 T}{\partial y^2} = \rho c_e \frac{\partial^2 T}{\partial t^2} + T_0\frac{\partial^2}{\partial t^2}\left(\beta_{11}\frac{\partial u}{\partial x} + \beta_{22}\frac{\partial v}{\partial y}\right) \tag{7}$$

$$\sigma_{11} = A_{11}\frac{\partial u}{\partial x} + A_{12}\frac{\partial v}{\partial y} - \beta_{11}(T - T_0) \tag{8}$$

$$\sigma_{22} = A_{12}\frac{\partial u}{\partial x} + A_{22}\frac{\partial v}{\partial y} - \beta_{22}(T - T_0) \tag{9}$$

$$\sigma_{12} = A_{13}\left(\frac{\partial v}{\partial x} + \frac{\partial u}{\partial y}\right) \tag{10}$$

where

$$A_{11} = \lambda + 2(\alpha + \mu_T) + 4(\mu_L - \mu_T) + \beta$$
$$A_{12} = \lambda + \alpha, \quad A_{13} = \mu_L, \quad A_{22} = \lambda + 2\mu_T$$
$$\beta_{11} = (2\lambda + 3\alpha + 4\mu_l - 2\mu_T + \beta)\alpha_{11} + (\lambda + \alpha)\alpha_{22} \tag{11}$$
$$\beta_{22} = (2\lambda + \alpha)\alpha_{11} + (\lambda + 2\mu_T)\alpha_{22}$$

in which α_{11} and α_{22} are coefficients of linear thermal expansion. For convenience, the following non-dimensional variables are used:

$$(x', y', u', v') = c\chi(x, y, u, v), \quad t' = c^2\chi t$$
$$T' = \frac{\beta_{11}(T - T_0)}{\rho c^2}, \quad \Omega' = \frac{\Omega}{c^2\chi}$$
$$(\sigma'_{11}, \sigma'_{12}, \sigma'_{22}, \sigma'_0) = \frac{1}{\rho c^2}(\sigma_{11}, \sigma_{12}, \sigma_{22}, \sigma_0) \tag{12}$$
$$c^2 = \frac{A_{11}}{\rho}, \quad \chi = \frac{\rho c_e}{K_{11}}$$

In terms of the non-dimensional quantities defined in Eq. (12), the above governing equations reduce to (dropping the dashed for convenience)

$$(1 + \sigma_0)\frac{\partial^2 u}{\partial x^2} + (B_1 + B_4)\frac{\partial^2 v}{\partial x \partial y} + (\sigma_0 + B_4)\frac{\partial^2 u}{\partial y^2}$$
$$= \frac{\partial T}{\partial x} + \frac{\partial^2 u}{\partial t^2} - \Omega^2 u - 2\Omega\frac{\partial v}{\partial t} \tag{13}$$

$$(B_4 + \sigma_0)\frac{\partial^2 u}{\partial x \partial y} + (B_1 + B_4)\frac{\partial^2 v}{\partial x^2} + (B_2 + \sigma_0)\frac{\partial^2 v}{\partial y^2}$$
$$= B_3\frac{\partial T}{\partial y} + \frac{\partial^2 v}{\partial t^2} - \Omega^2 v + 2\Omega\frac{\partial u}{\partial t} \tag{14}$$

$$\left(\varepsilon_2 + \varepsilon_3\frac{\partial}{\partial t}\right)\frac{\partial^2 T}{\partial x^2} + \left(\varepsilon_2 + \varepsilon\varepsilon_3\frac{\partial}{\partial t}\right)\frac{\partial^2 T}{\partial y^2}$$
$$= \frac{\partial^2 T}{\partial t^2} + \frac{\partial^2}{\partial t^2}\left(\varepsilon_0\frac{\partial u}{\partial x} + \varepsilon_1\frac{\partial v}{\partial y}\right) \tag{15}$$

$$\sigma_{11} = \frac{\partial u}{\partial x} + B_1\frac{\partial v}{\partial y} - T \tag{16}$$

$$\sigma_{22} = B_1\frac{\partial u}{\partial x} + B_2\frac{\partial v}{\partial y} - B_3 T \tag{17}$$

$$\sigma_{12} = B_4\left(\frac{\partial v}{\partial x} + \frac{\partial u}{\partial y}\right) \tag{18}$$

where

$$(B_1, B_2, B_4) = \frac{1}{A_{11}}(A_{12}, A_{22}, A_{13}), \quad B_3 = \frac{\beta_{22}}{\beta_{11}}$$
$$\varepsilon = \frac{K_{22}}{K_{11}}, \quad (\varepsilon_0, \varepsilon_1) = \frac{T_0\beta_{11}}{A_{11}\rho c_e}(\beta_{11}, \beta_{22}) \tag{19}$$
$$(\varepsilon_2, \varepsilon_3) = \frac{1}{\rho c_e}\left(\frac{K^*}{c^2}, K_{11}\chi\right)$$

3. APPLICATION

We consider the problem of a half-space Ψ, which is defined as follows:

$$\Psi = \{(x, y, z) : 0 \le x < \infty, -\infty < y < \infty, -\infty < z < \infty\} \tag{20}$$

The surface of the half-space is taken to be traction free, and the thermal shock $g(y, t)$ applied on the surface at $x = 0$ is taken of the form

$$g(y, t) = T_1 H(t) H(l - |y|) \tag{21}$$

where H is the Heaviside unit step function and T_1 is a constant. This means that heat is applied on the surface of the half-space on a narrow band of width $2l$ surrounding the y-axis to keep it at temperature T_1, while the rest of the surface is kept at zero temperature. Assuming the following initial conditions:

$$u = v = T = 0, \quad \dot{u} = \dot{v} = \dot{T} = 0, \quad \text{at } t = 0 \tag{22}$$

4. FINITE ELEMENT FORMULATION

The Finite element method is a powerful technique originally developed for numerical solution of complex problems in structural mechanics, and it remains the method of choice for complex systems. A further benefit of this method is that it allows physical effects to be visualized and quantified regardless of experimental limitations. On the other hand, the finite element method in different generalized thermoelastic problems has been applied by many authors (see for instant[22–26]).

In this section, the governing equations of generalized thermoelasticity based upon Green and Naghdi's theory are summarized, using the corresponding finite element equations. In the finite element method, the displacement components u, v and the temperature T are related to the corresponding nodal values by

$$u = \sum_{i=1}^{m} N_i u_i(t), \quad v = \sum_{i=1}^{m} N_i v_i(t), \quad T = \sum_{i=1}^{m} N_i T_i(t) \tag{23}$$

where m denotes the number of nodes per element, and N_i are the shape functions. The eight-node isoparametric, quadrilateral element is used for displacement components and temperature calculations. The weighting functions and the shape functions coincide. Thus,

$$\delta u = \sum_{i=1}^{m} N_i \delta u_i, \quad \delta v = \sum_{i=1}^{m} N_i \delta v_i, \quad \delta T = \sum_{i=1}^{m} N_i \delta T_i \tag{24}$$

It should be noted that appropriate boundary conditions associated with the governing equations, Eqs. (13)–(15) must be adopted in order to properly formulate a problem. Boundary conditions are either essential (geometric)

or natural (traction) types. Essential conditions are prescribed displacements u, v and temperature T while, the natural boundary conditions are prescribed tractions and heat flux. They expressed as

$$\sigma_{xx}n_x+\sigma_{xy}n_y=\bar{\tau}_x,\quad \sigma_{xy}n_x+\sigma_{yy}n_y=\bar{\tau}_y,\qquad q_xn_x+q_yn_y=\bar{q} \tag{25}$$

where n_x and n_y are direction cosines of the outward unit normal vector at the boundary, $\bar{\tau}_x$, $\bar{\tau}_y$ are the given tractions values, and $\bar{q}$ is the given surface flux.

In the absence of body force, the governing equations are multiplied by weighting functions and then are integrated over the spatial domain ϖ with the boundary Γ. Applying integration by parts and making use of the divergence theorem reduce the order of the spatial derivatives and allows for the application of the boundary conditions. Thus, the finite element equations corresponding to Eqs. (13)–(15) can be obtained as

$$\begin{aligned}
&\int_\Gamma \begin{Bmatrix} \delta u\bar{\tau}_x \\ \delta v\bar{\tau}_y \\ \delta T\bar{q} \end{Bmatrix} d\Gamma \\
&=\int_\varpi \begin{Bmatrix} \dfrac{\partial \delta u}{\partial x}\sigma_{xx}+\dfrac{\partial \delta u}{\partial y}\sigma_{xy} \\ \dfrac{\partial \delta v}{\partial x}\sigma_{xy}+\dfrac{\partial \delta v}{\partial y}\sigma_{yy} \\ \varepsilon_2\dfrac{\partial \delta T}{\partial x}\dfrac{\partial T}{\partial x}+\varepsilon_2\dfrac{\partial \delta T}{\partial y}\dfrac{\partial T}{\partial y} \end{Bmatrix} d\varpi \\
&+\int_\varpi \begin{Bmatrix} \delta u\left(\dfrac{\partial^2 u}{\partial t^2}-\Omega^2u-2\Omega\dfrac{\partial v}{\partial t}-\sigma_o\left(\dfrac{\partial^2 u}{\partial x^2}+\dfrac{\partial^2 u}{\partial y^2}\right)\right) \\ \delta v\left(\dfrac{\partial^2 v}{\partial t^2}-\Omega^2v+2\Omega\dfrac{\partial u}{\partial t}-\sigma_o\left(\dfrac{\partial^2 v}{\partial x^2}+\dfrac{\partial^2 v}{\partial y^2}\right)\right) \\ \delta T\left(\dfrac{\partial^2 T}{\partial t^2}+\dfrac{\partial^2}{\partial t^2}\left(\varepsilon_0\dfrac{\partial u}{\partial x}+\varepsilon_1\dfrac{\partial v}{\partial y}\right)-\varepsilon_3\dfrac{\partial}{\partial t}\left(\dfrac{\partial^2 T}{\partial x^2}+\varepsilon\dfrac{\partial^2 T}{\partial y^2}\right)\right) \end{Bmatrix} d\varpi
\end{aligned} \tag{26}$$

Substituting the constitutive relations Eqs. (16)–(18), and Eqs. (24) and (25) into Eq. (26) leads to

$$\begin{aligned}
&\sum_{e=1}^{me}\left(\begin{bmatrix} M_{11}^e & 0 & 0 \\ 0 & M_{22}^e & 0 \\ M_{31}^e & M_{32}^e & M_{33}^e \end{bmatrix}\begin{Bmatrix} \ddot{u}^e \\ \ddot{v}^e \\ \ddot{T}^e \end{Bmatrix}\right. \\
&+\begin{bmatrix} 0 & C_{12}^e & 0 \\ C_{21}^e & 0 & 0 \\ 0 & 0 & C_{33}^e \end{bmatrix}\begin{Bmatrix} \dot{u}^e \\ \dot{v}^e \\ \dot{T}^e \end{Bmatrix} \\
&\left.+\begin{bmatrix} K_{11}^e & K_{12}^e & K_{13}^e \\ K_{21}^e & K_{22}^e & K_{23}^e \\ 0 & 0 & K_{33}^e \end{bmatrix}\begin{Bmatrix} u^e \\ v^e \\ T^e \end{Bmatrix}=\begin{Bmatrix} F_1^e \\ F_2^e \\ F_3^e \end{Bmatrix}\right)
\end{aligned} \tag{27}$$

where me is the total number of elements. The coefficients in Eq. (27) are presented in Appendix A.

Symbolically, the discredited equations of Eq. (27) can be written as

$$M\ddot{d}+c\dot{d}+Kd=F^{\text{ext}} \tag{28}$$

where M, C, K, and F^{ext} represent the mass, damping, stiffness matrices, and external force vectors, respectively, $d=[u\,v\,T]^T$. On the other hand, the time derivatives of the unknown variables have to be determined by the Newmark time integration method (see Wriggers[27]).

5. NUMERICAL EXAMPLES

To illustrate the proposed finite element approach, the following physical constants for generalized fiber-reinforced thermoelastic materials are used.

$$\begin{gathered}
\lambda=5.65\times10^{10}\ \text{N}\cdot\text{m}^{-2},\quad \mu_T=2.46\times10^{10}\ \text{N}\cdot\text{m}^{-2} \\
\mu_L=5.66\times10^{10}\ \text{N}\cdot\text{m}^{-2},\quad \rho=2660\ \text{kg.m}^{-3} \\
\alpha=-1.28\times10^{10}\ \text{N}\cdot\text{m}^{-2},\quad \beta=220.90\times10^{10}\ \text{N}\cdot\text{m}^{-2} \\
\alpha_{11}=0.017\times10^{-4}\ \text{k}^{-1},\quad \alpha_{22}=0.015\times10^{-4}\ \text{k}^{-1} \\
c_e=0.787\times10^{3}\ \text{J}\cdot\text{kg}^{-1}\cdot\text{k}^{-1},\quad T_0=293\ \text{k},\quad l=0.5 \\
K_{11}=0.0921\times10^{3}\ \text{J}\cdot\text{m}^{-1}\cdot\text{s}^{-1}\cdot\text{k}^{-1},\quad T_1=1 \\
K_{22}=0.0963\times10^{3}\ \text{J}\cdot\text{m}^{-1}\cdot\text{s}^{-1}\cdot\text{k}^{-1}
\end{gathered}$$

To study the effect of reinforcement on wave propagation, some numerical examples are presented graphically. The numerical applications will be carried out for the displacements u and v, temperature T, and stresses σ_{11}, σ_{12} and σ_{22} that being reported herein at $y=0.5$, $t=0.2$, $T_1=1$, and for different values of initial stress σ_0 and angular velocity Ω.

The distributions of u, v, T, σ_{11}, σ_{12} and σ_{22} are presented in Figures 1–6 through the longitudinal x-direction for $\Omega=2$ and for different values of σ_0. All quantities, except the temperature, are very sensitive to the variation of the initial stress σ_0. As σ_0 increases the displacement v and the longitudinal stress σ_{11} increase while the displacement u decreases. The temperature may be independent of σ_0 while the values of the normal stress σ_{22} and in-plane stress σ_{12} oscillate randomly with distance x. The displacements vanish at $x=1.6$, the longitudinal stress σ_{11}

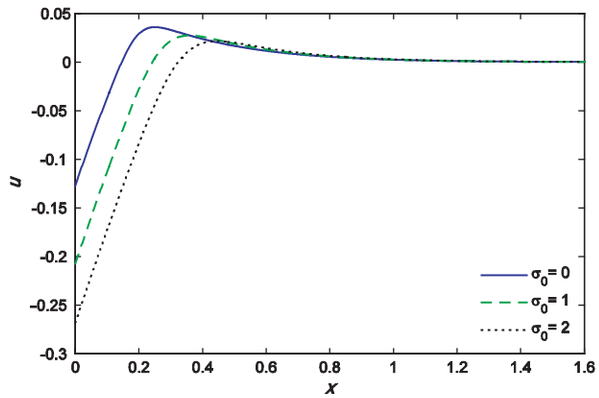

Fig. 1. Variation of horizontal displacement u with distance x.

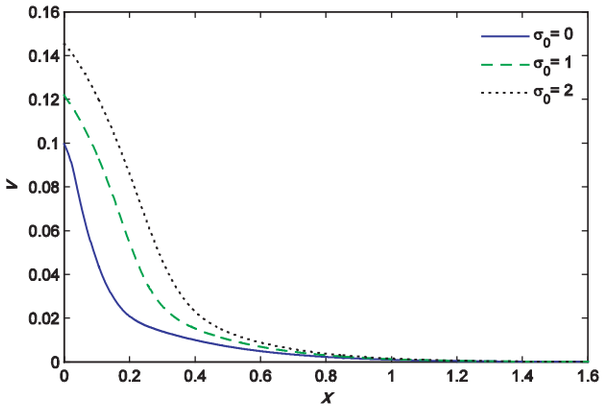

Fig. 2. Variation of vertical displacement v with distance x.

and the normal stress σ_{22} vanish at $x = 2.0$, the in-plane stress σ_{12} vanishes at $x = 1.5$, and the temperature vanishes at $x = 2.5$.

The effect of the angular velocity Ω is also discussed here. Similar plots for all quantities are presented in Figures 7–12 for $\sigma_0 = 1$ and different values of Ω.

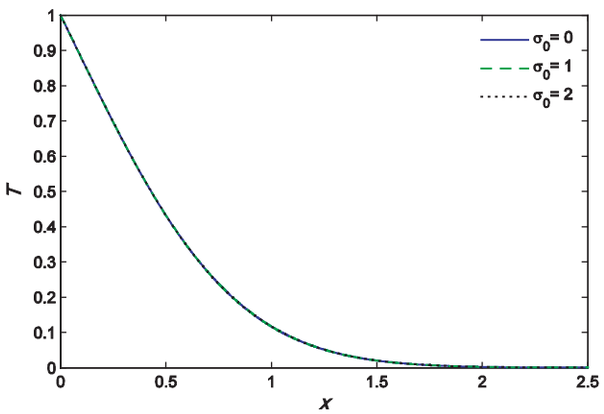

Fig. 3. Variation of temperature T with distance x.

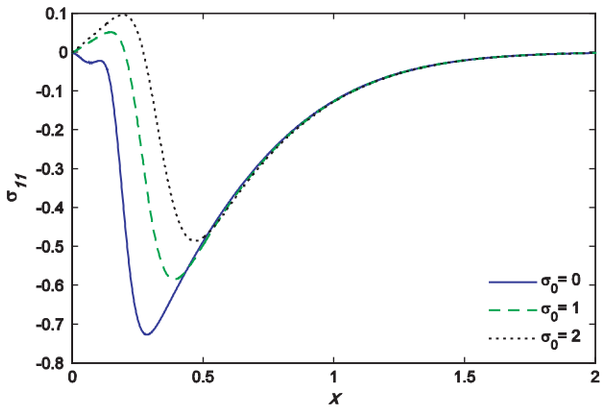

Fig. 4. Variation of stress component σ_{11} with distance x.

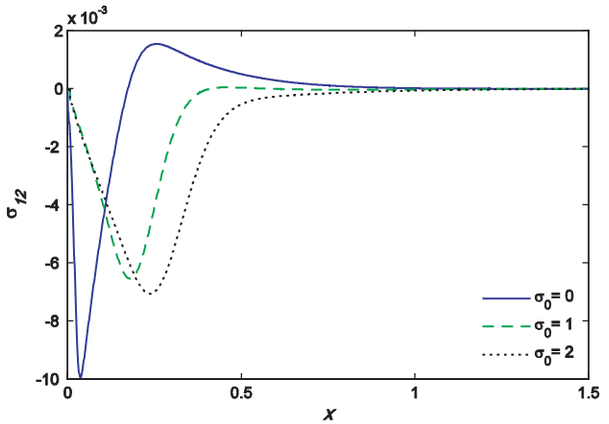

Fig. 5. Variation of stress component σ_{12} with distance x.

Figure 7 shows that the horizontal displacement u is no longer increasing and decreasing monotonically with maximum values at $0.3 < x < 0.5$. Figure 8 shows that the vertical displacement decreases directly as x increases. Both u and v reach to zero when $x = 1.5$. Once again,

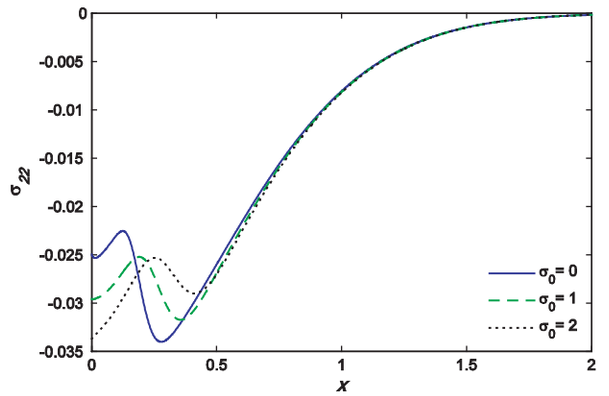

Fig. 6. Variation of stress component σ_{22} with distance x.

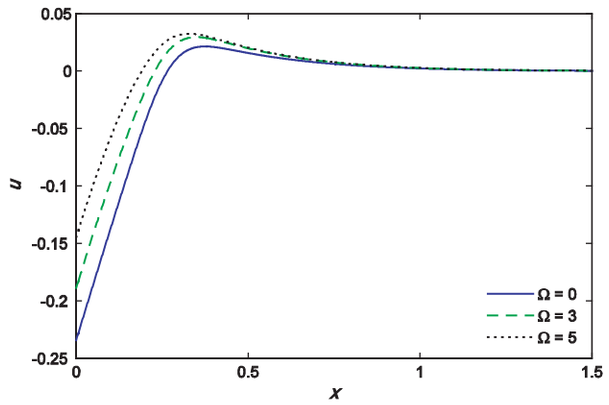

Fig. 7. Variation of horizontal displacement u with distance x.

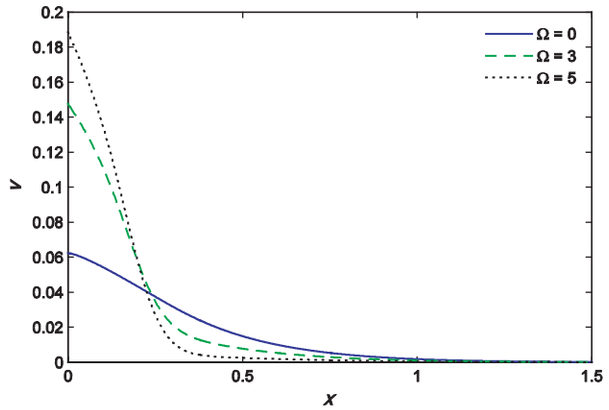

Fig. 8. Variation of vertical displacement v with distance x.

the temperature is independent of Ω and it decreases as x increases and vanishes when $x = 2.5$ as shown in Figure 9. The longitudinal stress σ_{11}, as shown in Figure 10, increases as Ω decreases and this irrespective to the value of x. The same behavior is illustrated by σ_{22} in Figure 12. The two stresses vanish when $x = 2.0$.

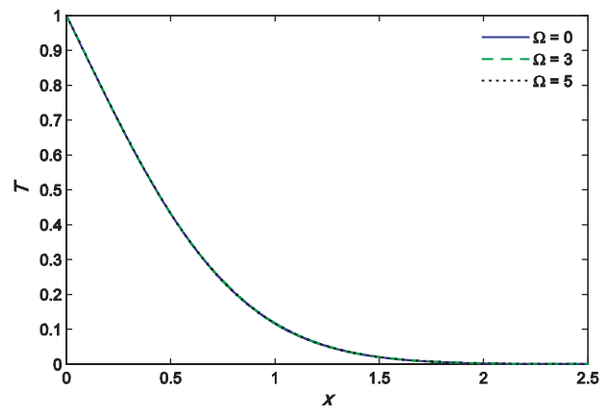

Fig. 9. Variation of temperature T with distance x.

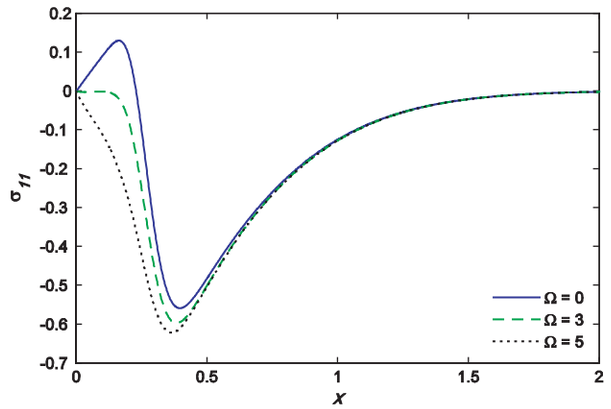

Fig. 10. Variation of stress component σ_{11} with distance x.

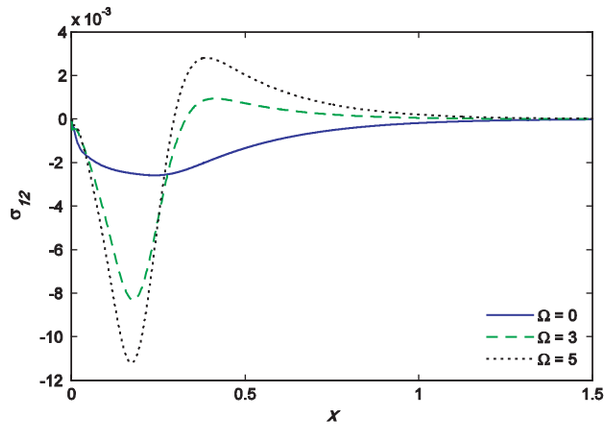

Fig. 11. Variation of stress component σ_{12} with distance x.

Also, Figure 11 shows that σ_{12} oscillate randomly with distance x and vanishes when $x = 1.5$.

Finally, the inclusion of the fiber-reinforcement coefficients is also discussed. The quantities of thermoelastic medium with fiber-reinforcements (WRE) and those without fiber-reinforcements (NRE) are presented in

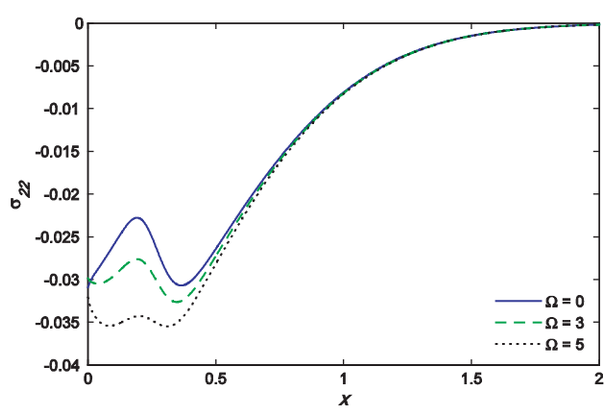

Fig. 12. Variation of stress component σ_{22} with distance x.

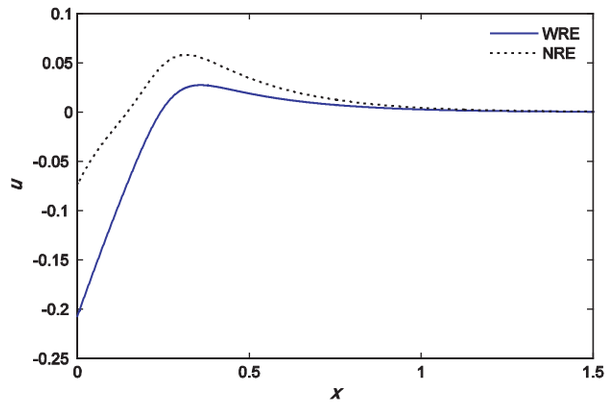

Fig. 13. Variation of horizontal displacement u with distance x.

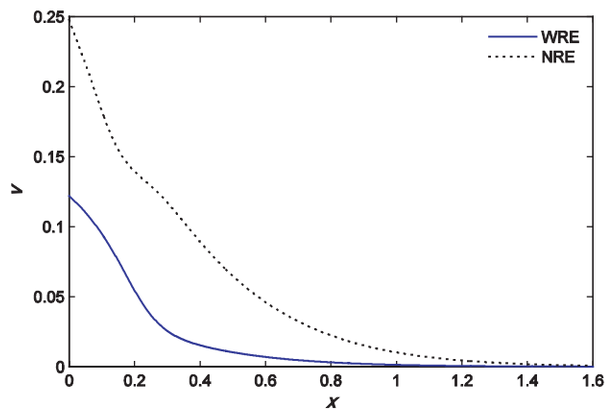

Fig. 14. Variation of vertical displacement v with distance x.

Figures 13–18 for $\sigma_0 = 1$ and $\Omega = 2$. It is observed that the variations of all quantities with fiber-reinforcements (WRE) are least oscillatory than the variations of all quantities without fiber-reinforcements (NRE).

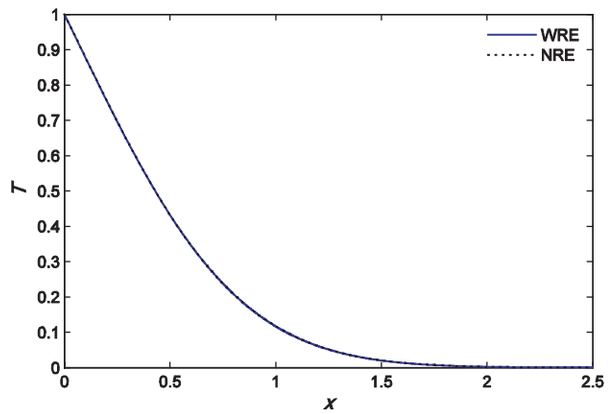

Fig. 15. Variation of temperature T with distance x.

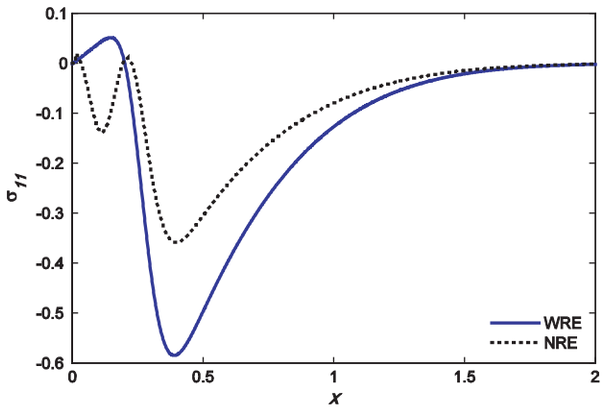

Fig. 16. Variation of stress component σ_{11} with distance x.

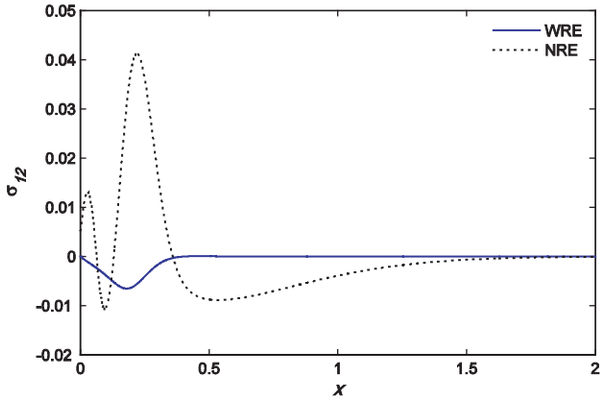

Fig. 17. Variation of stress component σ_{12} with distance x.

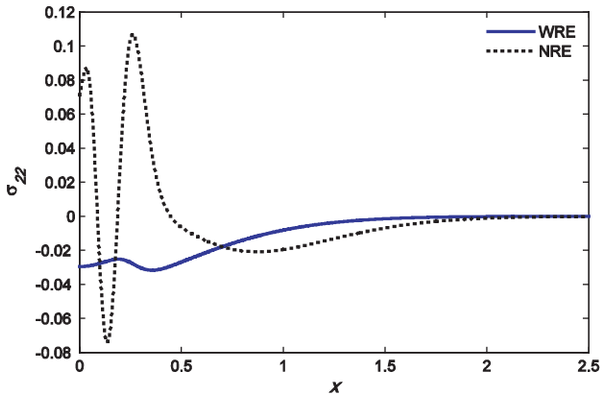

Fig. 18. Variation of stress component σ_{22} with distance x.

6. CONCLUSION

As observed of the plots of all quantities, the inclusion of the fiber-reinforcement coefficients, as well as the initial stress and rotation play an important role of deformation of the medium. The variations of displacements may be more uniform than those of stresses. However, the temperature still independent of all variables.

RESEARCH ARTICLE

APPENDIX A

The coefficients appeared in Eq. (27) are given by

$$M_{11}^e = \int_{\varpi} [N]^T [N]\, d\varpi, \quad C_{12}^e = \int_{\varpi} -2\Omega [N]^T [N]\, d\varpi$$

$$K_{11}^e = \int_{\varpi} \left(\left[\frac{\partial N}{\partial x}\right]^T \left[\frac{\partial N}{\partial x}\right] + B_4 \left[\frac{\partial N}{\partial y}\right]^T \left[\frac{\partial N}{\partial y}\right] - \sigma_o [N]^T \left[\frac{\partial^2 N}{\partial x^2} + \frac{\partial^2 N}{\partial y^2}\right] - \Omega^2 [N]^T [N] \right) d\varpi$$

$$K_{12}^e = \int_{\varpi} \left(B_1 \left[\frac{\partial N}{\partial x}\right]^T \left[\frac{\partial N}{\partial y}\right] + B_4 \left[\frac{\partial N}{\partial y}\right]^T \left[\frac{\partial N}{\partial x}\right] \right) d\varpi$$

$$K_{13}^e = \int_{\varpi} -\left[\frac{\partial N}{\partial x}\right]^T [N]\, d\varpi, \quad M_{22}^e = \int_{\varpi} [N]^T [N]\, d\varpi$$

$$C_{21}^e = \int_{\varpi} 2\Omega [N]^T [N]\, d\varpi$$

$$K_{21}^e = \int_{\varpi} \left(B_4 \left[\frac{\partial N}{\partial x}\right]^T \left[\frac{\partial N}{\partial y}\right] + B_1 \left[\frac{\partial N}{\partial y}\right]^T \left[\frac{\partial N}{\partial x}\right] \right) d\varpi$$

$$K_{22}^e = \int_{\varpi} \left(B_4 \left[\frac{\partial N}{\partial x}\right]^T \left[\frac{\partial N}{\partial x}\right] + B_2 \left[\frac{\partial N}{\partial y}\right]^T \left[\frac{\partial N}{\partial y}\right] - \sigma_o [N]^T \left[\frac{\partial^2 N}{\partial x^2} + \frac{\partial^2 N}{\partial y^2}\right] - \Omega^2 [N]^T [N] \right) d\varpi$$

$$K_{23}^e = \int_{\varpi} -B_3 \left[\frac{\partial N}{\partial y}\right]^T [N]\, d\varpi$$

$$M_{31}^e = \int_{\varpi} \varepsilon_0 [N]^T \left[\frac{\partial N}{\partial x}\right] d\varpi, \quad M_{32}^e = \int_{\varpi} \varepsilon_1 [N]^T \left[\frac{\partial N}{\partial y}\right] d\varpi$$

$$M_{33}^e = \int_{\varpi} [N]^T [N]\, d\varpi$$

$$C_{33}^e = \int_{\varpi} -\varepsilon_3 [N]^T \left(\left[\frac{\partial^2 N}{\partial x^2}\right] + \varepsilon \left[\frac{\partial^2 N}{\partial y^2}\right] \right) d\varpi$$

$$K_{33}^e = \int_{\varpi} \varepsilon_2 \left(\left[\frac{\partial N}{\partial x}\right]^T \left[\frac{\partial N}{\partial x}\right] + \left[\frac{\partial N}{\partial y}\right]^T \left[\frac{\partial N}{\partial y}\right] \right) d\varpi$$

$$F_1^e = \int_{\Gamma} [N]^T \bar{\tau}_x\, d\Gamma, \quad F_2^e = \int_{\Gamma} [N]^T \bar{\tau}_y\, d\Gamma$$

$$F_3^e = \int_{\Gamma} [N]^T \bar{q}\, d\Gamma$$

References

1. V. Danilovskaya, *Prikl. Mat. Mekh.* 14, 316 (**1950**).
2. M. Biot, *J. Appl. Phys.* 27, 240 (**1956**).
3. H. W. Lord and Y. Shulman, *J. Mech. Phys. Solids* 15, 299 (**1967**).
4. A. E. Green and K. A. Lindsay, *J. Elasticity* 2, 1 (**1972**).
5. J. Ignaczak, *J. Thermal Stresses* 2, 171 (**1979**).
6. R. S. Dhaliwal and A. Singh, Dynamic Coupled Thermoelasticity, Hindustan Publishing, New Delhi, India (**1980**).
7. R. S. Dhaliwal and H. Sherief, *Q. Appl. Math.* 3, 1 (**1980**).
8. D. S. Chandrasekharaiah, *Appl. Mech. Rev.* 39, 355 (**1986**).
9. A. E. Green and P. M. Naghdi, *J. Elasticity* 31, 189 (**1993**).
10. R. B. Hetnarski and J. Ignaczak, *Int. J. Solids Struct.* 37, 215 (**2000**).
11. A. S. El-Karamany and M. A. Ezzat, *Int. J. Eng. Sci.* 42, 649 (**2004**).
12. A. M. Zenkour, D. S. Mashat, and K. A. Elsibai, *Math. Problems Eng.* 1 (**2009**), Article ID 962351.
13. Z. Hashin and W. B. Rosen *J. Appl. Mech.* 31, 223 (**1964**).
14. P. R. Sengupta and S. Nath, *Sādhanā* 26, 363 (**2001**).
15. S. J. Singh, *Sādhanā* 26, 363 (**2001**); *Sādhanā* 27, 1 (**2002**).
16. H. H. Sherief and R. S. Dhaliwal, *J. Thermal Stresses* 4, 407 (**1981**).
17. R. S. Dhaliwal and J. G. Rokne, *J. Thermal Stresses* 11, 241 (**1989**).
18. H. Li and R. S. Dhaliwal, *Indian J. Pure Appl. Math.* 27, 85 (**1996**).
19. B. Singh, *Arch. Appl. Mech.* 75, 513 (**2006**).
20. Z. Qian, F. Jin, K. Kishimoto, and T. Lu, *Int. J. Solids Struct.* 46, 1354 (**2009**).
21. M. Schoenberg and D. Censor, *Q. Appl. Math.* 31, 115 (**1973**).
22. X. Tian, Y. Shen, C. Chen, and T. He, *Int. J. Solids Struct.* 43, 2050 (**2006**).
23. I. A. Abbas, *Int. J. Thermophys.* 33, 567 (**2012**).
24. I. A. Abbas and M. I. Othman, *Int. J. Thermophys.* 33, 913 (**2012**).
25. I. A. Abbas and A. N. Abd-Alla, *Arch. Appl. Mech.* 78, 283 (**2008**).
26. I. A. Abbas and M. Othman, *Chin. Phys. B* 21, 014601 (**2012**).
27. P. Wriggers, Nonlinear Finite Element Methods, Springer Berlin Heidelberg (**2008**).

Received: 30 October 2012. Accepted: 28 November 2012.